



HAL
open science

The mRNA-binding proteome of a critical phase transition during Arabidopsis seed germination

Nikita Sajeev, Anirban Baral, Antoine H.P. America, Leo A.J. Willems, Rémy Merret, Léonie Bentsink

► To cite this version:

Nikita Sajeev, Anirban Baral, Antoine H.P. America, Leo A.J. Willems, Rémy Merret, et al.. The mRNA-binding proteome of a critical phase transition during Arabidopsis seed germination. *New Phytologist*, In press, 10.1111/nph.17800 . hal-03377537

HAL Id: hal-03377537

<https://univ-perp.hal.science/hal-03377537>

Submitted on 14 Oct 2021

HAL is a multi-disciplinary open access archive for the deposit and dissemination of scientific research documents, whether they are published or not. The documents may come from teaching and research institutions in France or abroad, or from public or private research centers.

L'archive ouverte pluridisciplinaire **HAL**, est destinée au dépôt et à la diffusion de documents scientifiques de niveau recherche, publiés ou non, émanant des établissements d'enseignement et de recherche français ou étrangers, des laboratoires publics ou privés.



New Phytologist

The mRNA-binding proteome of a critical phase transition during *Arabidopsis* seed germination

Journal:	<i>New Phytologist</i>
Manuscript ID	NPH-MS-2021-37074.R1
Manuscript Type:	MS - Regular Manuscript
Date Submitted by the Author:	24-Sep-2021
Complete List of Authors:	Sajeev, Nikita; Wageningen Universiteit en Research, Plant Physiology Baral, Anirban; Wageningen Universiteit en Research, Plant Physiology America, Antoine H.P. ; Wageningen Universiteit en Research, BU Bioscience Willems, Leo; Wageningen Universiteit en Research, Plant Physiology Merret, Rémy; Universite de Perpignan Via Domitia, LGDP UMR5096 Bentsink, Leónie; Wageningen Universiteit en Research, Plant Physiology
Key Words:	mRNA, RNA binding proteins, Seeds, Translation, Germination

SCHOLARONE™
Manuscripts

1 **The mRNA-binding proteome of a critical phase transition during Arabidopsis seed**
 2 **germination**

3 Nikita Sajeev¹, Anirban Baral¹, Antoine H.P. America², Leo A.J. Willems¹, Rémy Merret³
 4 and Leónie Bentsink^{1*}

5

6 ¹Wageningen Seed Science Centre, Laboratory of Physiology Wageningen University,
 7 6708PB Wageningen, The Netherlands

8 ²BU Bioscience, Wageningen Plant Research, 6700 AP Wageningen, The Netherlands

9 ³Laboratoire Génome et Développement des Plantes, CNRS-LGDP UMR 5096, 66860
 10 Perpignan, France

11

12 *Author for correspondence:

13 Leónie Bentsink

14 Email: leonie.bentsink@wur.nl

Total word count (excluding summary, references, acknowledgements and legends):	6407	Acknowledgements	59
Summary:	189	No. of figures	5
Introduction:	732	No. of tables	0
Materials and Methods:	2449	No. of Supporting Information files:	2
Results and discussion	3186		

15

16 **Abstract**

- 17 • *Arabidopsis thaliana* seed germination is marked by extensive translational control
18 at two critical phase transitions. The first transition refers to the start of hydration,
19 the hydration translational shift. The second shift, the germination translational
20 shift (GTS) is the phase between testa rupture and radicle protrusion at which the
21 seed makes the all or nothing decision to germinate.
- 22 • The mechanism behind the translational regulation at these phase transitions is
23 unknown. RNA binding proteins are versatile players in the post-transcriptional
24 control of mRNAs and as such candidates for regulating translation during seed
25 germination.
- 26 • Here, we report the mRNA binding protein repertoire of seeds during the GTS.
27 Thirty seed specific RBPs and 22 dynamic RBPs were identified during the GTS,
28 like the putative RBP Vacuolar ATPase subunit A and RBP HSP101. Several stress
29 granule markers were identified in this study, which suggests that seeds are
30 prepared to quickly adapt the translation of specific mRNAs in response to changes
31 in environmental conditions during the GTS.
- 32 • Taken together this study provides a detailed insight into the world of RNA binding
33 proteins during seed germination and their possible regulatory role during this
34 developmentally regulated process.

35 **Keywords**

36 Germination, mRNA, RNA binding proteins, seeds, translation.

37

38 **Introduction**

39 Seed germination is a complex process in which the seeds need to undergo developmental
40 transitions to successfully establish themselves as a plant. The majority of our
41 understanding on how plant development is regulated has been a product of studying gene
42 expression with the main focus on transcription and DNA binding partners. However,
43 recent studies have highlighted that translational regulation plays an important role in
44 regulating plant development (Sorenson & Bailey-Serres, 2014; Merchante *et al.*, 2017;
45 Sablok *et al.*, 2017; Cho *et al.*, 2018; Cho *et al.*, 2019; Jang *et al.*, 2019). The complete
46 switch-off state of translation between seed maturation and seed germination makes seeds
47 a unique system to study developmentally regulated translation (Sajeev *et al.*, 2019).
48 Previously, it has been shown that there is extensive translational control at two temporal
49 shifts during seed germination. These shifts were defined as the hydration translation shift
50 (HTS) and germination translational shift (GTS) (Bai *et al.*, 2017). Interestingly these shifts
51 coincide with important developmental phase transitions during seed germination. The
52 HTS spans the first six hours after imbibition (HAI); the phase at which seeds take up
53 water. Upon imbibition, the dry seed undergoes a drastic transition from a metabolically
54 inactive to a highly active state. The GTS is the developmental phase between seed testa
55 rupture (TR) and radicle protrusion (RP). These phases mark critical physiological stages
56 of seed germination. Upon TR, seeds can still be dried back without hampering its viability
57 which becomes more difficult as germination progresses. This is because desiccation
58 tolerance can be re-introduced into seeds only within a limited time frame which is usually
59 lost once upon RP (Maia *et al.*, 2011). This developmental transition can be viewed as a
60 point of no return, also known as germination *sensu strictu* (Perino & Côme, 1991). The
61 decision to germinate is based on a complex web of environmental and developmental
62 signals to ensure seedling survival. At the GTS, distinct subsets of mRNAs show
63 differential translation which suggests dynamic regulation of germination (Bai *et al.*,
64 2017). The mechanism behind this selection is yet to be understood. In recent years, several
65 studies have implicated RNA binding proteins (RBPs) can regulate their target mRNAs co-
66 and post-transcriptionally, thereby altering its translation efficiency in plants (Köster *et al.*,
67 2017; Lou *et al.*, 2020). Furthermore, a recent study reported that certain stored mRNAs
68 in the dry seed are associated with single ribosomes and RBPs which are later
3

69 translationally upregulated during germination (Bai *et al.*, 2020). This led to the hypothesis
70 that certain RBPs could play a role in determining the fate of the regulated mRNAs during
71 seed germination.

72 Defining features of RBPs are their putative RNA binding domains like the Pumilio (PUM)
73 domain, Zinc-finger domains, K homology (KH) domain or the RNA recognition motif
74 (RRM) (Lorković, 2009). Several studies have demonstrated the role of RBPs in plant
75 development. Some examples include the RBP JULGI that regulates phloem
76 differentiation by translational control of *SUPPRESSOR OF MAX2-LIKE1-4/5 (SMXL4/5)*
77 and *ETHYLENE INSENSITIVE2 (EIN2)* a non-canonical RBP that can regulate hypocotyl
78 elongation by repressing the translation of ethylene responsive mRNAs ((Merchante *et al.*,
79 2015; Cho *et al.*, 2018; Cho *et al.*, 2019). In seeds, through a transcriptomics study, an RBP
80 belonging to the PUM family, *ARABIDOPSIS PUMILIO (APUM) 9* was shown to play a
81 role in delaying seed germination (dormancy) (Xiang *et al.*, 2014). Although, recent
82 advancements in RNA-protein interactome capture techniques have allowed the
83 identification of classical and novel RNA binding proteins (RBPs) in different plant tissues,
84 their identity and role in seeds has not yet been explored (Maronedze *et al.*, 2016; Reichel
85 *et al.*, 2016; Zhang *et al.*, 2016; Köster *et al.*, 2017; Cho *et al.*, 2019; Bach-Pages *et al.*,
86 2020).

87 In the present study, mRNA interactome capture was performed in Arabidopsis embryos
88 at TR and RP, the physiological stages that mark the GTS. Hundreds of high confidence
89 RBPs were identified. Additionally, dynamic RBPs were identified in this study like the
90 putative RBP Vacuolar H⁺-ATPase subunit A and known RBP HEAT SHOCK PROTEIN
91 101 (HSP101). These RBPs were also exclusively identified in the seed mRNA interactome
92 capture and not in leaves, protoplasts or etiolated seedlings (Maronedze *et al.*, 2016;
93 Reichel *et al.*, 2016; Zhang *et al.*, 2016; Bach-Pages *et al.*, 2020). Overall, this study
94 provides a valuable resource for future RBP research in seeds and will be the starting point
95 of identifying their possible regulatory role in translation during seed germination.

96

97 **Results and discussion**

98 **Identification of the mRNA binding proteome at the germination translational shift**

99 The GTS defines the period of translational regulation between TR and RP. The exact
100 moment of RP is genotype and environment dependent, which implies that this has to be
101 determined for every new experiment. In this experiment, TR and RP occurred at 26 and
102 42 hours after imbibition (HAI) for Arabidopsis ecotype Col-0 seeds (Fig. S1). To unravel
103 the mRNA binding proteome during the GTS, the existing mRNA binding interactome
104 protocol had to be extensively adapted for Arabidopsis embryos (Castello *et al.*, 2013) (Fig.
105 1a). The mRNA interactome capture was performed on the embryos of three independent
106 biological replicates at TR and RP. To summarize, UV radiation was used to crosslink (CL)
107 the mRNA-RBP complexes while processing the non-crosslinked controls (NCL) in
108 parallel. The embryos were lysed in a denaturing buffer and poly-A mRNA was pulled
109 down using oligo- dT magnetic beads (Fig. 1a). Poly-A mRNA enrichment was seen in the
110 eluates after poly-A pulldown compared to the total input RNA before pulldown using
111 qPCR (Fig. S2). Next, the enrichment of proteins in the CL samples over the NCL was
112 confirmed using silver stained SDS-PAGE gels (Fig. 1b). The samples were then analyzed
113 using label free nano LC MS/MS analysis. Scatter plots of the LFQ (Relative Label-free
114 quantitation) intensities between the replicates showed good reproducibility at both time-
115 points (Fig. S3).

116 Over 1300 proteins were identified across all samples. However, only proteins for which
117 two or more unique peptides were detected in at least two biological replicates of the CL
118 samples were taken for further analysis. This resulted in more than 600 proteins that were
119 enriched in the CL samples in both stages. One hundred and six and 112 proteins were
120 identified as high confidence RBPs (FDR<5%) at TR and RP respectively (GTS-RBPs),
121 with an overlap of 54 proteins that were present at both time-points (Supporting
122 Information Table S1a,b). Although, several proteins did not pass these stringent
123 parameters of selection, many proteins were highly enriched in the crosslinked samples
124 over the controls and therefore could be important RBPs that play a role in the GTS. Hence,
125 228 proteins at TR and 244 proteins at RP with a log₂ fold (CL/NCL) enrichment >1 were

126 classified into a second set called the candidate RBPs for each time-point in our dataset
127 (Fig. 1c and Table S1a,b).

128 Next, the GTS-RBPs and candidate RBPs were annotated based on their molecular
129 function. This revealed that approximately 80% of the GTS-RBPs had been previously
130 annotated with known or predicted RNA binding activity, while 47 GTS-RBPs were not
131 and could be putative RBPs (Fig 1d). The candidate RBP set showed a large proportion of
132 RBPs not annotated as mRNA binding and therefore provide a repertoire of putative RBPs
133 in seeds (Fig. 1d, S1a,b). A gene ontology (GO) enrichment analysis for all GTS and
134 candidate RBPs over the two time-points showed common enrichment for GO terms like
135 binding, mRNA binding, heterocyclic compound binding and organic cyclic compound
136 binding (Table S1c). Overall, the GO analysis, revealed that the interactome capture
137 strongly enriched for proteins related to RNA biology.

138 **Protein domain analysis reveals stage specific protein families during the GTS**

139 Both the GTS-RBPs and candidate RBPs at TR and RP were grouped by their protein
140 domain annotations (PFAM or Interpro annotations) (Fig. 2a, Table S1d). At both stages,
141 diverse classical and non-classical RNA binding domains (RBDs) were captured (Fig. 2a).
142 Examples of classical domains include RRM, KH domain, Zinc finger (zf)-CCCH, DEAD
143 box Helicases and PUM. The vast majority of the RBPs identified contained the RRM
144 domain (Fig. 2a). The Arabidopsis proteome consists of 253 proteins containing an RRM
145 domain (Lorković & Barta, 2002). The RRM family is highly diverse in plants and in this
146 study 66 GTS-RBPs and 47 candidate RBPs containing an RRM domain were identified
147 in seeds. Majority of the RRMs have not been investigated for their roles in germination
148 and could be important regulators of germination. An example of such a regulator is an
149 RRM containing glycine rich protein, atRZ-1a, which was identified as a candidate RBP
150 at RP. This RBP has been reported to negatively impact germination under salt and osmotic
151 stress (Kim *et al.*, 2007). The Arabidopsis PUM family contains 25 proteins that are
152 phylogenetically classified into four groups. Interestingly only group 1 APUM RBPs
153 (APUM1,3,5 and 6) were identified as GTS-RBPs at both stages indicating that group 1
154 APUMs are especially abundant during seed germination.

155 Non-classical RBDs like Ribosomal, La and GTP-EFTU were also well represented at both
156 TR and RP (Fig. 1a). The non-classical RBD, HABP4_PAI-RBP1 family was only
157 identified in the candidate RBP set at TR (Fig. 2a). Three Hyaluronan/mRNA binding
158 proteins contained this RBD namely, AtRGGA, AT5G47210 and AT4G17520. AtRGGA
159 has been reported to play a role in abscisic acid (ABA) signalling during stress response in
160 seedlings. Mutants of this RBP are highly susceptible to salt and osmotic stress
161 (Ambrosone *et al.*, 2015). *AT5G47210* was revealed to be highly expressed one day after
162 seed imbibition followed by a reduction at later time-points (Narsai *et al.*, 2011). These
163 time-points closely coincide with the stages of TR and RP and could explain why this
164 protein is no longer identified at RP point. In the present study, one knockout mutant (Fig.
165 S4) and 2 complementation lines of *AT5G47210* have been investigated for seed
166 germination phenotypes. This revealed a dormancy phenotype, measured as DSDS50 (days
167 of seed dry storage required for 50% germination (Alonso-Blanco *et al.*, 2003; Soppe &
168 Bentsink, 2020). The knockout mutant *at5g47210* had a DSDS50 of only 8.5 days in
169 comparison to its wild type Col-0 which required 20 days (Fig. 2c). The complementation
170 lines COMP1 and COMP2, complemented this mutant phenotype (Fig. 2c). Therefore,
171 *AT5G47210* could play a role in inhibiting germination. The mechanism by which this
172 RBP regulates germination needs to be further explored.

173 The domain analysis also revealed many putative RBDs many of which belonged to the
174 elongation Initiation factor 3 (EIF3) family (Fig. 2b). Other protein families such as
175 HSP70, AAA and DUF1264 have also been identified as putative RBDs in previous studies
176 (Reichel *et al.*, 2016; Bach-Pages *et al.*, 2020). Interestingly, many enzyme families like
177 Phosphoglycerate kinase (PGK), thioredoxins, Glutathione-S-transferase (GST), and
178 NAD(P) binding domain (NAD(P)-bd_dom_sf) proteins were pulled down in this study
179 (Fig 2b, Table S1d). There have been more reports on metabolic enzymes with RNA
180 binding functions in eukaryotes (Castello *et al.*, 2015; Maronedze *et al.*, 2016; Reichel *et al.*,
181 2016; Bach-Pages *et al.*, 2020). PGKs and Thioredoxins have been validated as RBPs
182 in humans and yeast cells (Beckmann *et al.*, 2015). In plants, it has been shown that GSTs
183 are modulated by atRZ-1a, an RRM and Zinc finger domain containing protein also
184 identified as a GTS-RBP in this study. This report concluded that this enzyme among others

185 play a role in ROS homeostasis during germination (Kim *et al.*, 2007). In another study,
186 some NAD(P) binding domain proteins were identified as RBPs that respond to osmotic
187 stress (Marondedze *et al.*, 2019). Most enzyme families identified in this interactome
188 capture have been known to play a role in ROS homeostasis. However, their discovery as
189 a putative RBDs in this study, suggests novel roles for these metabolic enzymes as RBPs
190 in the translational regulation of seed germination.

191 **Dynamic RBPs identified during the GTS**

192 An in-depth analysis into the non-overlapping GTS- RBPs (106 at TR and 112 at RP)
193 showed that many RBPs were identified as a GTS-RBP at one time-point and as a candidate
194 RBP in the other. However, only 22 RBPs of these GTS- RBPs were exclusively identified
195 in one time-point alone and therefore classified as dynamic GTS-RBPs (Table S2). The
196 dynamic GTS-RBPs included known RBPs like ETHYLENE INSENSITIVE 2 (EIN2) and
197 HSP101 (Merchante *et al.*, 2015; Merret *et al.*, 2017). EIN2 mutants have been shown to
198 have a very strong dormancy phenotype due to high ABA levels in the dry seed (Koorneef
199 *et al.*, 2002). This study demonstrates that EIN2 can also function as an RBP during seed
200 germination. HSP101 was reported to bind and regulate the translation of the internal light-
201 regulatory element (iLRE) of ferredoxin (Fed-1) mRNA in carrot protoplasts (Ling *et al.*,
202 2000). A recent study further showed that HSP101 is required for the efficient release of
203 ribosomal protein mRNAs from stress granules for the rapid recovery of the translational
204 machinery from heat stress (Merret *et al.*, 2017). Traditionally, HSP proteins are regarded
205 as conserved molecular chaperones involved in protein folding stability and activation.
206 However, several other HSPs such as HSP81.2, HSP70 and HSP70b were identified as part
207 of the candidate RBP set at TR while HSP60, HSP91 chloroplast and mitochondria
208 HSP70.1 were identified in the candidate RBP dataset at the RP stage. HSP101 was the
209 only GTS RBP identified exclusively at the TR point and could function as an RBP
210 involved in the phase transition from TR to RP, however the *hsp101* mutant did not show
211 a germination or dormancy phenotype compared to wild-type (Fig. S5).

212 We also identified many dynamic putative GTS-RBPs. An example of a dynamic GTS-
213 RBP with no links to RNA biology is the VACUOLAR H⁺-ATPase SUBUNIT A (V-
214 ATPase SUBUNIT A) identified at the RP stage. V-ATPases are versatile multi-subunit

215 proton pumps that control the pH of many intracellular compartments in all eukaryotic
216 cells. In Arabidopsis, V-ATPases play a role in plant defenses against environmental
217 stresses like salt stress. The subunit A gene detected in Arabidopsis can produce at least
218 four different transcripts by using different polyadenylation sites. These transcripts differ
219 only in their 3' untranslated region and produce identical proteins (Magnotta & Gogarten,
220 2002).

221 The dynamic nature and the RBP identity for HSP101 and V-ATPase SUBUNIT A was
222 validated using western blotting (Fig. 3a). ARGONAUTE 1 (AGO1) being a well-
223 established RBP also identified in this study was used as a positive control and ACTIN 7
224 was used as a negative control (Fig. 3a). The results confirmed the dynamic nature of
225 HSP101 and V-ATPase SUBUNIT A which were highly abundant in the CL samples at
226 TR and RP respectively (Fig. 3a, Fig. S6). Although AGO1 showed similar LFQ intensities
227 at TR and RP in this study, the western blot showed some dynamics for this protein
228 indicating the qualitative rather than quantitative nature of label free proteomics. The
229 negative control ACTIN 7 was only present in the total protein of TR and RP and not after
230 the poly-A pulldown, demonstrating the stringency of the mRNA interactome procedure.
231 To confirm that the changes observed after the interactome capture were not due to
232 differences in total protein abundance, an additional proteomics analysis on the total input
233 protein fractions was performed at both stages. As highly abundant proteins can limit the
234 identification of less abundant proteins, we were able to identify only 11 out of the 22
235 dynamic GTS-RBPs in the total input protein samples (Table S1f, Table S2). The data
236 confirmed that there were no significant differences in protein abundance for HSP101 and
237 V-ATPase SUBUNIT A at TR and RP before the interactome capture. This further supports
238 our hypothesis that HSP101 and V-ATPase SUBUNIT A are dynamic RBPs at TR and RP
239 respectively.

240 HSP101 plays a role in releasing ribosomal RNAs from stress granules for heat stress
241 recovery (Maia *et al.*, 2011; Merret *et al.*, 2017). In the case of V-ATPase SUBUNIT A,
242 its function as an RBP is unclear. It has been previously reported that vacuoles from tomato
243 protoplasts can contain RNA oligonucleotides (Abel *et al.*, 1990) and a recent study
244 demonstrated that, RNase T2 ribonucleases are targeted to vacuoles for rRNA degradation

245 and maintenance of cellular homeostasis in Arabidopsis (Floyd *et al.*, 2017). Both these
246 studies show that RNAs can be targeted to vacuoles. A plausible hypothesis could be that
247 putative GTS-RBP V-ATPase SUBUNIT A is involved in the sequestration of RNA to the
248 expanding vacuoles at RP to maintain cellular RNA homeostasis. However, further
249 research is required to establish the RBP identity and roles of both these RBPs during the
250 GTS.

251 **Comparison with other plant interactome captures reveal seed specific RBPs**

252 Due to technical advancements in the recent years, mRNA interactome capture has gained
253 a momentum in plant research. In the last five years, four different studies have published
254 the mRNA interactome of Arabidopsis seedlings (300 RBPs), leaves (717 and 230 RBPs)
255 and protoplasts (325 RBPs) (Maronedze *et al.*, 2016; Reichel *et al.*, 2016; Zhang *et al.*,
256 2016; Bach-Pages *et al.*, 2020). Although the previous studies identified much larger sets
257 of statistically enriched RBPs, a comparative analysis of all GTS-RBPs identified in this
258 study with previously performed interactome captures revealed 30 GTS-RBPs that were
259 only identified in germinating seeds and 5 RBPs that were common to all datasets (Fig. 3b,
260 Table S1e and S3). This shows that Arabidopsis RBPs are highly versatile, tissue and
261 developmental stage specific. Eleven out of these 30 seed specific GTS RBPs had been
262 previously annotated with an mRNA binding function and contained classical RNA
263 binding domains. Many previously unknown RBPs in this set were enzymes like H (+)-
264 ATPase 1, pyruvate orthophosphate di-kinase and hydroxysteroid dehydrogenase 5 (Fig.
265 3b, Table S3). Interestingly, nine out of the 30 seed specific RBPs are also part of the
266 dynamic GTS-RBPs set identified in this study.

267 **Stress granule markers enable quick responses to the environment**

268 During the GTS the seed makes an all or nothing decision to germinate or not. In a
269 biological context, germination must only proceed when the environmental conditions
270 allow the successful establishment of the seedling. Several proteins that have been
271 previously described to be part of cytoplasmic stress granules were identified at both stages
272 with similar LFQ intensities like, RNA BINDING PROTEIN 47 A (RBP47), RBP47B,
273 OLIGOURIDYLATE-BINDING PROTEIN 1C (AtUBP1c) and POLY-A BINDING
274 PROTEIN 2 (PABP2). Stress granules are cytoplasmic foci which are formed in response

275 to various environmental stresses like salt stress, hypoxia and heat stress (Chantarachot &
276 Bailey-Serres, 2018). Stress granules can transiently store mRNAs until the stress resolves,
277 allowing cells to quickly repress the translation of specific mRNAs in a stressful situation.
278 To show that stress granule markers quickly respond to stressful conditions, a reporter line
279 of stress granule marker RFP-PABP2 was imaged at TR and RP in response to heat stress
280 (Fig. 4b). At control conditions PABP2 was expressed throughout the cytoplasm in the
281 radicle tip of embryos and did not show any clear foci formation. Interestingly, after a short
282 heat stress, PABP2 is clearly localized into cytoplasmic stress granules at both TR and RP
283 (Fig. 4a). Further, to explore whether dynamic GTS-RBP HSP101 could regulate
284 translation at TR, PABP2 was imaged in *hsp101* background after a short heat stress. (Maia
285 et al., 2011; Merret et al., 2017). As expected, the number of stress granules in the *hsp101*
286 seeds were significantly higher than wild-type at the TR stage (Fig. S7) suggesting that
287 HSP101 is a GTS-RBP that could play a role in the translational control of germination via
288 stress granules. This suggests that seeds during GTS possibly express certain stress granule
289 markers in preparation for a quick adaptation of translation in response to changed
290 environmental conditions.

291 P-bodies are also cytoplasmic granules in which translationally repressed mRNAs can be
292 decayed or stored for development or stress responses (Narsai *et al.*, 2011; Hubstenberger
293 *et al.*, 2017). P-bodies can contain several RBPs, 5' to 3' exoribonucleases, de-adenylation
294 factors and factors involved in nonsense-mediated mRNA decay (Maldonado Bonilla,
295 2014). Some examples of P-body components are DECAPPING PROTEIN 1 (DCP1),
296 DCP2, DCP5 and EXORIBONUCLEASE4 (XRN4) (Xu & Chua, 2009). Although, many
297 of these P-body makers are known to be expressed in seeds, we only identified DCP5 as a
298 dynamic GTS-RBP at the TR point. Previously, DCP5, has been shown to play a role in
299 the translational repression of mRNAs via P-bodies in seedlings and in dark/light phase
300 translation (Xu & Chua, 2009). To explore the localization of DCP5 during the GTS, a
301 DCP5-GFP reporter line was imaged at TR and RP (Fig 4a). At TR, DCP5 forms more
302 cytoplasmic granules than at the RP stage in the epidermal cells of the radicle tip (Fig. 4b).
303 This differential localization could explain why DCP5 was identified as a dynamic GTS-
304 RBP in the present study. Interestingly, DCP5 was the only well-established P-body marker

305 identified in the interactome capture of leaves and in seedlings (Reichel *et al.*, 2016; Bach-
306 Pages *et al.*, 2020) while for example, DCP1 was not. This indicates that the mRNA
307 interactome capture method may not be an ideal to pull down all types of cytoplasmic
308 granules. This could be explained by the fact that P-bodies contain deadenylation factors
309 that degrade the poly-A tails of the mRNAs and in the present interactome capture, only
310 poly-A mRNAs were pulled down (Maldonado Bonilla, 2014) or it could be that the
311 mRNAs present in these bodies are not easily accessible to the oligo-dT beads used in this
312 study.

313 In summary, the GTS spans a critical phase during germination at which extensive
314 translational regulation takes place in which 195 and 717 mRNAs are translationally up
315 and down regulated respectively (Bai *et al.*, 2017) (Fig. 5). The mechanism behind this
316 selection is yet to be elucidated. The fate of the regulated mRNAs could be controlled by
317 RBPs present during this shift. Over 600 GTS and candidate RBPs were identified. Among
318 these, 228 and 244 GTS-RBPs were identified with high confidence at TR and RP
319 respectively, 22 revealed to be dynamic GTS-RBPs and 30 were seed specific RBPs.
320 Several GTS-RBPs have been previously reported to play a role in Arabidopsis seed
321 germination. GTS-RBP EIN2 plays a role in reducing seed dormancy, possibly by
322 repressing the translation of mRNAs that promote dormancy via P-bodies, while HSP101
323 and COLD SHOCK PROTEIN 2 (CSP2) promote germination under abiotic stresses
324 (Hong & Vierling, 2001; Koornneef *et al.*, 2002; Park *et al.*, 2009; Li *et al.*, 2015). As
325 mentioned above, the GTS is marked by mRNAs that are translationally down regulated
326 (Bai *et al.*, 2017). These could be mRNAs that are remnants from maturation, storage
327 proteins or proteins that inhibit germination and thus needs to be degraded (Xu *et al.*, 2006).
328 DCP5 may play a role in the decay of these mRNAs via P-bodies during the GTS especially
329 as the RP as larger granules were observed at this stage (Fig 4b) (Xu & Chua, 2009).
330 Additionally, several stress granule markers were identified including the TUDOR-SN
331 protein (TSN1/2) and PABP2. TSN1/2 has been implied to promote seed germination
332 under salt stress by modulating the mRNA levels of the key GA biosynthesis enzyme
333 *GA20ox3* (Liu *et al.*, 2010). Stress granule marker PABP2 formed stress granules after a
334 short heat stress. Other GTS-RBPs, like APUM5, COLD SHOCK PROTEIN 1 (CSP1) and

335 AtRZ1 have been reported to negatively regulate germination under abiotic stress
336 conditions (Kim *et al.*, 2007; Park *et al.*, 2009; Huh & Paek, 2014). The presence of RBPs
337 that repress translation or inhibit germination during the GTS, may indicate that during
338 germination, seeds are prepared for quick responses to environmental changes. All together
339 this study provides the first step towards understanding the role of RBPs in the translational
340 control of mRNAs during the GTS, which is important to ensure successful radicle
341 protrusion and thereby completion of germination.

For Peer Review

342 **Materials and Methods**

343 **Plant materials**

344 Fully after ripened seeds of *Arabidopsis thaliana* accession Columbia-0 (Col-0) were used
345 for all assays described in this manuscript (NASC N60000). The mutant line of
346 Hyaluronan/mRNA binding protein (AT5G47210) was obtained from NASC
347 (SALKseq_055953). The complementation lines contain the genomic fragment (forward
348 primer AGGAGGAGGAGGAGAGAA and reverse primer:
349 TCGCAGAAAAGACCTTCA) with its native promoter transferred to the mutant
350 backgrounds using entry vector pDONR207 and the destination vector pKGW-RedSeed
351 (<https://gatewayvectors.vib.be/collection/pkgw-redseed>). The pPABP2-PABP2-RFP
352 reporter lines in wild type and *hsp101* background were described in Merret et al., 2017.
353 The pUBQ-DCP5-GFP like was a kind gift from the lab of Scheer, H el ene (Scheer *et al.*,
354 2021) while the *hsp101* mutant and complementation line used for the germination
355 phenotypes of Fig S5 were a kind gift from Elizabeth Vierling (McLoughlin *et al.*, 2019).

356 **Germination condition and assays**

357 Seeds were sowed on two layers of blue blotter paper (Anchorpaper company,
358 www.seedpaper.com) were equilibrated with 48ml of demineralized water in plastic trays
359 (15X21cm). Each replicate contained 1.2g of seeds which were wrapped in a closed
360 transparent plastic bag and placed at 22 C in continuous light (143 m m-2s-1) for
361 germination. The time-points for the germination translational shift were selected based on
362 the physiological stage of the seeds described previously (7). In this study TR occurred at
363 26 hours after imbibition (HAI) and RP at 42 HAI.

364 To determine the DSDS50 values, germination assays were carried from 3 days until 5
365 weeks after harvest, when the seeds were fully after-ripened (100% germination). The
366 germination experiments were performed as described above, however at 26 C instead of
367 at 22 C, since these suboptimal germination conditions allowed to also identify smaller
368 differences in dormancy level (Alonso-Blanco *et al.*, 2003). The germination percentages
369 were calculated using the germinator software package (Joosen *et al.*, 2010) and the
370 DSDS50 levels were calculated using the statistical program R version 2.14 (R
371 Development Core Team, 2009; www.r-project.org) (He *et al.*, 2014).

372 Embryo isolation and UV crosslinking

373 For embryo isolation, the imbibed seeds were scraped from the tray and pressed between
374 two microscope slides. Due to the pressure applied, the embryos were expelled out of the
375 seed coat. The embryo-seed coat mixture was separated in a 40% sucrose solution. Using
376 centrifugation, the mixture was separated and the top layer containing the pure embryos
377 was collected. The embryos were spread evenly over a germination tray containing white
378 Whatmann filter papers to absorb the sucrose solution (Lopez-Molina, personal
379 communication).

380 For in-vivo crosslinking (CL), the trays were placed on ice and irradiated in a Stratalinker
381 (Stratagene) with 254nm UV light at 1J/cm². The crosslinking was performed twice with
382 30 seconds pause in between treatments. The controls were processed simultaneously. The
383 embryos were harvested immediately after irradiation and frozen in liquid N₂.

384 The frozen embryo tissue was ground into fine powder in liquid N₂ and resuspended in
385 tubes with 24 ml of a modified seed RBP extraction buffer (1.25% Sucrose, 400mM Tris-
386 HCl pH 8, 0.5% LiDS, 200mM LiCl, 35mM MgCl₂, 1mM EGTA, 5mM DTT, 20U/ml
387 RNasin, 1X EDTA-free Complete Protease cocktail inhibitor tablet). The tubes containing
388 the lysate were placed on ice for 10 minutes following which they were centrifuged for 20
389 minutes at 14000 rpm to precipitate the cell debris. The supernatant (20ml) from each tube
390 was transferred to fresh RNase free tube. Aliquots from the lysate were taken for quality
391 controls (silver stain, western blots) and for mRNA enrichment check.

392 The mRNA-protein complexes were isolated using 1.5 ml of oligo(dT)25 magnetic beads
393 (New England Biolabs) per tube. The beads were equilibrated using 5ml of wash buffer 1
394 (20mM Tris-HCl pH 7.6, 0.1% LiDS, 500mM LiCl, 1mM EDTA, 5mM DTT) and
395 incubated for 2 minutes with gentle rotation at 4°C. The tubes were placed on the magnetic
396 rack, which resulted in the magnetic capture of the beads and a clear suspension. Thereafter
397 the supernatant of the magnetic beads was discarded and the cell lysate was immediately
398 added to the tubes and incubated at 4°C for 1 hour by applying gentle rotation. Beads were
399 collected on the magnet and washed twice with 15mL of ice-cold wash buffer1, buffer 2
400 (20mM Tris-HCl pH 7.6, 500mM LiCl, 1mM EDTA, 5mM DTT) and wash buffer 3
401 (20mM Tris-HCl pH 7.6, 200mM LiCl, 1mM EDTA, 5mM DTT) for 5 mins at room
15

402 temperature. Finally, the beads were incubated with 500 μ L of elution buffer (20mM Tris-
403 HCl pH 7.6, 1mM EDTA) at 50°C for 3 minutes to release the poly(A)-tailed RNAs from
404 the beads. Two additional rounds of pulldown were performed for each sample, and the
405 three eluates were combined in a new RNase free tube (total volume 1.5 ml).

406 **mRNA enrichment check using qRT-PCR**

407 Aliquots taken of the total Input and after poly-A pulldown samples were spiked with a
408 mix of the four eukaryotic poly(A) RNAs (Affymetrix, Santa Clara, CA, USA; Ambion,
409 P/N900433), and purified with TriPure Isolation Reagent (Roche, Basel, Switzerland).
410 cDNA was synthesized using the iScript™ cDNA synthesis kit (Bio-Rad, Hercules, CA,
411 USA) according to the manufacturer's protocol. qRT-PCR was performed using Power
412 SYBR Green (Applied Biosystems, Waltham MA, USA) in a 10 μ l reaction using the
413 standard program of the ViiA™ 7 instrument (Applied Biosystems). To quantify RNA
414 levels, the comparative Ct method, namely the $2^{-\Delta\Delta Ct}$ method was used and normalized
415 to the geometric mean of the spike-in standards (Livak & Schmittgen, 2001).

416 **RNA Quantification and Normalization for SDS page loading**

417 The pooled eluates were quantified using the NanoDrop spectrophotometer (260/280 ratios
418 between 1.7-2.0). All samples were normalized for mRNA quantity in both time-points and
419 for each replicate using the elution buffer.

420 **RNase treatment and Protein concentration**

421 The mRNA was digested by adding 100 units of the commercially available RNase cocktail
422 containing RNase A and T1 to the eluates. The samples were mixed and incubated at 37°C
423 for 1 hour along with a negative control sample. After the RNase digestion the samples
424 were concentrated using Amicon® centrifugal filter units (0.5mL, 3kDa). Each sample was
425 concentrated to approximately 40 μ L in low-binding Eppendorf tubes.

426 **SDS-PAGE, Silver Staining and Immunoblot**

427 20 μ L of the concentrated protein samples mixed with of 5x SDS loading dye were loaded
428 on a 12% Bis-Tris protein gel (Thermo Fisher). The gel was run at 100V until the loading
429 dye reached the end of the resolving gel. The SDS page gel was washed twice with ultra-
430 pure water for 5 minutes each time. The silver staining was performed using LCMS-MS
431 compatible silver staining protocol (34).

432 For western blotting, following the SDS-PAGE, the gels were electroblotted on to PVDF
433 membranes (Trans-Blot Turbo Mini 0.2 μ m PVDF transfer packs, BIO-RAD). The
434 membranes were blocked with 5% nonfat milk in 1x TBST (1x TBS with 0.1% Tween 20)
435 for 1 hour at room temperature, followed by an overnight incubation at 4°C with primary
436 antibodies in 3% nonfat milk with rotation. The membrane was incubated with secondary
437 in 3% nonfat milk in 1x TBST for 1 hour at room temperature. Protein signals were
438 detected using a high sensitivity ECL substrate and visualized using the Chemidoc (BIO-
439 RAD). The primary antibodies used were Anti-AGO1 (Agrisera; AS09-527), Plant Anti-
440 Actin (Agrisera; AS13 2640), Anti-HSP101 (Kind gift from Elizabeth Vierling, Amherst,
441 Massachusetts) and Anti- V-ATPase subunit A (Agrisera; AS09467). The secondary
442 Antibody used was HRP-conjugated Anti-Rabbit IgG concentrate (Item I1) (Sigma
443 Aldrich; RABHRP1).

444 **Sample Preparation for Proteomics**

445 The gel lanes were cut out per sample. The lanes were cut such that it did not include the
446 RNase enzyme bands present in the lane. Each lane was cut into tiny pieces and divided
447 equally over 3 Eppendorf tubes. The gel pieces were washed with milliQ water and 100%
448 Acetonitrile (ACN). For reduction and alkylation, the gel pieces were incubated with 100
449 μ L of 10mM DTT in 50mM Ammonium bicarbonate (pH 7.6) at 56°C for 45 minutes. The
450 samples were brought back to room temperature. Supernatant was removed and gel pieces
451 were washed with 50% ACN. Following this, 100 μ L of 54mM iodoacetamide was added
452 to the gel pieces. The tubes were incubated at room temperature for 20 minutes in the dark.
453 The gel pieces were washed three times using 100% ACN and Ammonium bicarbonate
454 alternatively. After the last wash with ACN, the gel pieces were shortly dried on air and
455 then incubated overnight with 10ng of trypsin in 50mM Ammonium bicarbonate (pH 7.6)
456 at 37°C for protein digestion. The next day the peptides were extracted from the gel twice
457 with 50 μ L 50% ACN and 100% ACN. Next, the pooled extracts were vacuum dried for
458 2h and the dried pellets were dissolved in 0.1% formic acid and used for MS.

459 For the Input total protein samples, 50 μ g of the lysate was used in a total volume of 25 μ L.
460 Following this step 3 μ L of iodoacetamide was added to lysate and incubated at room

461 temperature for 20 minutes in the dark. Next, 3 μ L of 12% phosphoric acid was added to the
462 sample. To prepare lysates that contain detergents like Lithium dodecyl sulphate for nana-
463 LCLMS/MS, the the S-Trap™ Micro spin columns= digestion protocol was used
464 (<https://protifi.com/pages/s-trap>) according to the manufacturer's protocol. An overnight
465 on column protein digestion was performed on the samples, using 1.5 μ g of trypsin in
466 50mM Ammonium bicarbonate (pH 7.6) at 37°C. The next day the peptides were eluted
467 from the columns with 35 μ L of 50% ACN and 0.2% formic acid. Next, the pooled extracts
468 were vacuum dried for 2h and the dried pellets were dissolved in 0.1% formic acid and
469 used for MS.

470 **Liquid Chromatography-Tandem MS Analysis**

471 Samples were analyzed on an LTQ-Orbitrap Velos Pro mass spectrometer (Thermo
472 Scientific) coupled to a nanoAcquity UPLC system (Waters). Peptides were loaded onto a
473 trapping column (nanoAcquity Symmetry C18, 5 μ m, 180 μ m \times 20 mm) at a flow rate of
474 15 μ L/min with solvent A (0.1% formic acid). Peptides were separated over an analytical
475 column (nanoAcquity BEH C18, 1.7 μ m, 75 μ m \times 200 mm) at a constant flow of 0.3
476 μ L/min using the following gradient: 3% solvent B (acetonitrile and 0.1% formic acid) for
477 10 min, 7 to 25% solvent B within 210 min, 25 to 40% solvent B within 10 min, and 85%
478 solvent B for 10 min. Peptides were introduced into the mass spectrometer using a Pico-
479 Tip Emitter (360 μ m outer diameter \times 20 μ m inner diameter, 10 μ m tip; New
480 Objective). MS survey scans were acquired from 300 to 1700 m/z at a nominal resolution
481 of 30,000. The 15 most abundant peptides were isolated within a 2D window and subjected
482 to tandem MS (MS/MS) sequencing using collision-induced dissociation in the ion trap
483 (activation time, 10 ms; normalized collision energy, 40%). Only 2+/3+ charged ions were
484 included for analysis. Precursors were dynamically excluded for 30 s (exclusion list size
485 was set to 500)

486 **Peptide and protein Identification**

487 Raw data were processed using MaxQuant (version 1.6.1) (Cox & Mann, 2008).MS/MS
488 spectra were searched against the Araport11 Arabidopsis database (input proteome version
489 11/07/2015 including 50.164 entries) concatenated to a database containing protein
490 sequences of common contaminants. Enzyme specificity was set to trypsin/P, allowing a
18

491 maximum of two missed cleavages. Cysteine carbamidomethylation was set as fixed
492 modification, and methionine oxidation and protein N-terminal acetylation were used as
493 variable modifications. The minimal peptide length was set to six amino acids and a
494 minimum of one unique peptide was required for the identification. The mass tolerances
495 were set to 20 ppm for the first search, 6 ppm for the main search, and 0.05 Da for product
496 ion masses. FDRs for peptide and protein identification were set to 1%. Match between
497 runs (time window 2 min) and requantify options were enabled, as well as the IBAQ
498 function.

499 **Definition of GTS-RBPs and Candidate RBPs**

500 The proteinGroups.txt output from MaxQuant was further processed in Perseus version
501 1.6.12 from MaxQuant (Tyanova *et al.*, 2016). Proteins that were identified in at least 2 or
502 more biological replicates of the CL treatment and with a minimum of 2 unique peptides
503 identified the proteins were selected for further analysis. To be able to perform statistics
504 between the NCL and CL samples, all normalized LFQ intensities were log₂ transformed
505 and the missing values were replaced by a constant minimum value of 10. Next, t-tests
506 were performed with a Benjamin-Hochberg correction for multiple t-testing and a false
507 discovery rate of 5% between the NCL and CL for each stage. Proteins that were
508 statistically enriched in the CL samples were defined as the GTS-RBPs per time-point and
509 the ones that were not statistically enriched but had a log₂ fold (CL/NCL) ≥ 1, were defined
510 as the candidate RBP set per stage. Similar analysis was performed for the Input total
511 protein. Here only the LFQ intensities of all proteins identified in the CL Input total protein
512 samples were compared between the TR and RP stages.

513 **GO and PFAM Annotation and Analysis**

514 GO and PFAM Annotation for the proteins was performed using the Perseus tool (version
515 1.6.12) (Tyanova *et al.*, 2016) using the GO database and PFAM database plugins. Proteins
516 that contained the term RNA binding in their GO annotation were categorized as the 'RNA
517 binding' set. PFAM classification was done on the RNA binding and Not binding set by
518 counting the number of proteins per protein family in each stage. The proteins were
519 classified as classical or non-classical RBPs based on previous reports. GO enrichment
520 analysis was performed using the g:Profiler tool (<http://biit.cs.ut.ee/gprofiler/>) (Raudvere
521 *et al.*, 2019) using the Arabidopsis genome as a reference dataset. For statistical t-tests,

522 Benjamin Hochberg correction for multiple testing was chosen with 0.05 as the
523 significance level.

524 **Confocal Image Analysis**

525 For visualization of all reporter lines used in this study, epidermal cells from embryonic
526 root tips (at testa rupture and radical protrusion stages imbibed in water) were imaged with
527 a Leica SP8 laser scanning confocal microscope equipped with 63X oil immersion
528 objective (NA 1.4). For the heat stress treatment, embryos were excised and exposed to a
529 short heat stress of 42°C in water for 30 minutes before loading onto a slide for
530 visualization under the Leica SP8 confocal microscope. YFP and RFP fluorophores were
531 excited with 488nm and 552 nm laser lines, respectively and their fluorescence emissions
532 were collected in 515-550 nm and 580-650 nm windows respectively. For each category,
533 30 epidermal cells from 5 seedlings were measured (n = 30). The number of granules were
534 quantified using Image J plugin 3D object counter (Du *et al.*, 2011). Maximum intensity
535 of a Z projection covering a depth of 5µm deep from the cell surface was quantified.
536 Particles with mean intensity in the upper 10th percentile and within a diameter range of
537 20-100 pixels were measured. The data was plotted as number of granules per 1000µm³
538 volume, the data normality was checked by Kolmogorov-Smirnov test and variance
539 equality was checked by Levene's test. (***) indicate p < 0.001 (Student t test).

540 **Supporting Information**

541 Additional supporting information may be found in the online version of this article.

542 **Fig. S1** Germination curve of the Col-0 seeds used to determine the GTS time-points

543 **Fig. S2** qRT-PCR depicting mRNA enrichment after poly-A pulldown of mRNAs at the
544 radicle protrusion stage of seed germination

545 **Fig. S3** Correlation plots between replicates for CL samples at Testa Rupture and Radicle
546 protrusion stages of Arabidopsis seed germination.

547 **Fig. S4** Confirmation of knockout mutant *at5g47210* using qRT-PCR

548 **Fig. S5** Germination of *hsp101* mutant under control conditions.

549 **Fig. S6** Confirmation of dynamic GTS-RBPs by western blotting.

550 **Fig. S7** Visualization of heat stress granule marker PABP2 in Col-0 and the *hsp101* mutant
551 at Testa Rupture.

552 **Table S1a** RNA binding proteins identified at testa rupture (TR) stage of the germination
553 translational shift

554 **Table S1b** RNA binding proteins identified at Radicle protrusion (RP) stage of the
555 germination translational shift.

556 **Table S1c** GO enrichment analysis based on Molecular function of the GTS and candidate
557 RNA binding proteins identified at Testa rupture and Radicle protrusion stages of
558 Arabidopsis seed germination

559 **Table S1d** Protein family classification of RNA binding proteins at testa rupture and
560 radicle protrusion stages of the germination translational shift

561 **Table S1e** Dataset showing RBPs that are unique and/or overlap between 5 different
562 interactome captures as shown in Figure 3

563 **Table S1f** Dataset showing all proteins identified in Input total protein samples at TR and
564 RP

565 **Table S2** Dynamic GTS-RBPs at testa Rupture and radicle protrusion during the
566 germination translational shift of seed germination

567 **Table S3** Seed specific RNA binding proteins identified by comparison with previously
568 performed interactome captures in *Arabidopsis thaliana*

569 **Acknowledgments**

570 This work is part of the research domain Applied and Engineering Sciences, project
571 number 15228, which is financed by the Dutch Research Council (NWO). This study is set
572 within the framework of the "Laboratoires d'Excellences (LABEX)" TULIP (ANR-10-
573 LABX-41) and of the "École Universitaire de Recherche (EUR)" TULIP-GS (ANR-18-

574 EURE-0019). We thank Dominique Gagliardi (IBMP, France) for providing GFP-DCP5
575 transgenic line.

576 **Author contribution**

577 NS and LB planned and designed the research. NS, AB, AHPA, LAJW performed
578 experiments. RM provided transgenic lines. NS and LB wrote the manuscript. All authors
579 commented on the manuscript.

For Peer Review

580 **References**

- 581 **Abel S, Blume B, Glund K. 1990.** Evidence for RNA-Oligonucleotides in Plant Vacuoles
582 Isolated from Cultured Tomato Cells. *Plant Physiology* **94**: 1163-1171.
- 583 **Alonso-Blanco C, Bentsink L, Hanhart CJ, Blankestijn-de Vries H, Koornneef M.**
584 **2003.** Analysis of natural allelic variation at seed dormancy loci of *Arabidopsis*
585 *thaliana*. *Genetics* **164**: 711-729.
- 586 **Ambrosone A, Batelli G, Nurcato R, Aurilia V, Punzo P, Bangarusamy DK, Ruberti**
587 **I, Sassi M, Leone A, Costa A, et al. 2015.** The *Arabidopsis* RNA-Binding Protein
588 AtRGGG Regulates Tolerance to Salt and Drought Stress. *Plant Physiology* **168**:
589 292-306.
- 590 **Bach-Pages M, Homma F, Kourelis J, Kaschani F, Mohammed S, Kaiser M, van der**
591 **Hoorn RA, Castello A, Preston GM. 2020.** Discovering the RNA-Binding
592 Proteome of Plant Leaves with an Improved RNA Interactome Capture Method.
593 *Biomolecules* **10**: 661.
- 594 **Bai B, Peviani A, Horst S, Gamm M, Bentsink L, Hanson J. 2017.** Extensive
595 translational regulation during seed germination revealed by polysomal profiling.
596 *New Phytologist* **214**: 233-244.
- 597 **Bai B, Van Der Horst S, Cordewener JH, America TA, Hanson J, Bentsink L. 2020.**
598 Seed-stored mRNAs that are specifically associated to monosomes are
599 translationally regulated during germination. *Plant Physiology* **182**: 378-392.
- 600 **Beckmann BM, Horos R, Fischer B, Castello A, Eichelbaum K, Alleaume A-M,**
601 **Schwarzl T, Curk T, Foehr S, Huber W. 2015.** The RNA-binding proteomes
602 from yeast to man harbour conserved enigmRBPs. *Nature communications* **6**: 1-9.
- 603 **Castello A, Hentze MW, Preiss T. 2015.** Metabolic enzymes enjoying new partnerships
604 as RNA-binding proteins. *Trends in Endocrinology & Metabolism* **26**: 746-757.
- 605 **Castello A, Horos R, Strein C, Fischer B, Eichelbaum K, Steinmetz LM, Krijgsveld**
606 **J, Hentze MW. 2013.** System-wide identification of RNA-binding proteins by
607 interactome capture. **8**: 491-500.
- 608 **Chantarachot T, Bailey-Serres J. 2018.** Polysomes, Stress Granules, and Processing
609 Bodies: A Dynamic Triumvirate Controlling Cytoplasmic mRNA Fate and
610 Function. *Plant Physiology* **176**: 254-269.

- 611 **Cho H, Cho HS, Hwang I. 2019.** Emerging roles of RNA-binding proteins in plant
612 development. *Current opinion in plant biology* **51**: 51-57.
- 613 **Cho H, Cho HS, Nam H, Jo H, Yoon J, Park C, Dang TVT, Kim E, Jeong J, Park S,**
614 **et al. 2018.** Translational control of phloem development by RNA G-quadruplex–
615 JULGI determines plant sink strength. *Nature Plants* **4**: 376-390.
- 616 **Cox J, Mann M. 2008.** MaxQuant enables high peptide identification rates, individualized
617 ppb-range mass accuracies and proteome-wide protein quantification. *Nature*
618 *biotechnology* **26**: 1367-1372.
- 619 **Du G, Drexler GA, Friedland W, Greubel C, Hable V, Krücken R, Kugler A, Tonelli**
620 **L, Friedl AA, Dollinger G. 2011.** Spatial dynamics of DNA damage response
621 protein foci along the ion trajectory of high-LET particles. *Radiation Research* **176**:
622 706-715.
- 623 **Floyd BE, Mugume Y, Morriss SC, MacIntosh GC, Bassham DC. 2017.** Localization
624 of RNS2 ribonuclease to the vacuole is required for its role in cellular homeostasis.
625 *Planta* **245**: 779-792.
- 626 **He H, de Souza Vidigal D, Snoek LB, Schnabel S, Nijveen H, Hilhorst H, Bentsink L.**
627 **2014.** Interaction between parental environment and genotype affects plant and
628 seed performance in Arabidopsis. *Journal of experimental botany* **65**: 6603-6615.
- 629 **Hong S-W, Vierling E. 2001.** Hsp101 is necessary for heat tolerance but dispensable for
630 development and germination in the absence of stress. *The Plant Journal* **27**: 25-
631 35.
- 632 **Hubstenberger A, Courel M, Bénard M, Souquere S, Ernoult-Lange M, Chouaib R,**
633 **Yi Z, Morlot J-B, Munier A, Fradet M. 2017.** P-body purification reveals the
634 condensation of repressed mRNA regulons. *Molecular cell* **68**: 144-157. e145.
- 635 **Huh SU, Paek K-H. 2014.** APUM5, encoding a Pumilio RNA binding protein, negatively
636 regulates abiotic stress responsive gene expression. *BMC plant biology* **14**: 75.
- 637 **Jang G-J, Yang J-Y, Hsieh H-L, Wu S-H. 2019.** Processing bodies control the selective
638 translation for optimal development of Arabidopsis young seedlings. *Proceedings*
639 *of the National Academy of Sciences* **116**: 6451-6456.

- 640 **Joosen RV, Kodde J, Willems LA, Ligterink W, van der Plas LH, Hilhorst HW. 2010.**
641 GERMINATOR: a software package for high-throughput scoring and curve fitting
642 of Arabidopsis seed germination. *The Plant Journal* **62**: 148-159.
- 643 **Kim Y-O, Pan S, Jung C-H, Kang H. 2007.** A Zinc Finger-Containing Glycine-Rich
644 RNA-Binding Protein, atRZ-1a, Has a Negative Impact on Seed Germination and
645 Seedling Growth of Arabidopsis thaliana Under Salt or Drought Stress Conditions.
646 *Plant and Cell Physiology* **48**: 1170-1181.
- 647 **Koornneef M, Bentsink L, Hilhorst H. 2002.** Seed dormancy and germination. *Current*
648 *opinion in plant biology* **5**: 33-36.
- 649 **Köster T, Maronedze C, Meyer K, Staiger D. 2017.** RNA-binding proteins revisited–
650 the emerging Arabidopsis mRNA interactome. *Trends in plant science* **6**: 512-526.
- 651 **Li W, Ma M, Feng Y, Li H, Wang Y, Ma Y, Li M, An F, Guo H. 2015.** EIN2-Directed
652 Translational Regulation of Ethylene Signaling in Arabidopsis. *Cell* **163**: 670-683.
- 653 **Ling J, Wells DR, Tanguay RL, Dickey LF, Thompson WF, Gallie DR. 2000.** Heat
654 shock protein HSP101 binds to the Fed-1 internal light regulatory element and
655 mediates its high translational activity. *The Plant Cell* **12**: 1213-1227.
- 656 **Liu S, Jia J, Gao Y, Zhang B, Han Y. 2010.** The AtTudor2, a protein with SN-Tudor
657 domains, is involved in control of seed germination in Arabidopsis. *Planta* **232**:
658 197-207.
- 659 **Livak KJ, Schmittgen TD. 2001.** Analysis of relative gene expression data using real-
660 time quantitative PCR and the $2^{-\Delta\Delta CT}$ method. *Methods* **25**(4): 402-408.
- 661 **Lorković ZJ. 2009.** Role of plant RNA-binding proteins in development, stress response
662 and genome organization. *Trends in plant science* **14**: 229-236.
- 663 **Lorković ZJ, Barta A. 2002.** Genome analysis: RNA recognition motif (RRM) and K
664 homology (KH) domain RNA-binding proteins from the flowering plant
665 Arabidopsis thaliana. *Nucleic acids research* **30**: 623-635.
- 666 **Lou L, Ding L, Wang T, Xiang Y. 2020.** Emerging Roles of RNA-Binding Proteins in
667 Seed Development and Performance. *International journal of molecular sciences*
668 **21**(18): 6822.

- 669 **Magnotta SM, Gogarten JP. 2002.** Multi site polyadenylation and transcriptional
670 response to stress of a vacuolar type H⁺-ATPase subunit A gene in *Arabidopsis*
671 *thaliana*. *BMC plant biology* **2**: 3.
- 672 **Maia J, Dekkers BJ, Provart NJ, Ligterink W, Hilhorst HW. 2011.** The re-
673 establishment of desiccation tolerance in germinated *Arabidopsis thaliana* seeds
674 and its associated transcriptome. *PloS one* **6**: e29123.
- 675 **Maldonado Bonilla LD. 2014.** Composition and function of P bodies in *Arabidopsis*
676 *thaliana*. *Frontiers in plant science* **5**:201.
- 677 **Maronedze C, Thomas L, Gehring C, Lilley KS. 2019.** Changes in the *Arabidopsis*
678 RNA-binding proteome reveal novel stress response mechanisms. *BMC plant*
679 *biology* **19**: 1-11.
- 680 **Maronedze C, Thomas L, Serrano NL, Lilley KS, Gehring C. 2016.** The RNA-binding
681 protein repertoire of *Arabidopsis thaliana*. *Scientific reports* **6**: 29766.
- 682 **McLoughlin F, Kim M, Marshall RS, Vierstra RD, Vierling E. 2019.** HSP101 Interacts
683 with the Proteasome and Promotes the Clearance of Ubiquitylated Protein
684 Aggregates. *Plant Physiology* **180**: 1829-1847.
- 685 **Merchante C, Brumos J, Yun J, Hu Q, Spencer KR, Enríquez P, Binder BM, Heber**
686 **S, Stepanova AN, Alonso JM. 2015.** Gene-specific translation regulation
687 mediated by the hormone-signaling molecule EIN2. *Cell* **163**: 684-697.
- 688 **Merchante C, Stepanova AN, Alonso JM. 2017.** Translation regulation in plants: an
689 interesting past, an exciting present and a promising future. *The Plant Journal* **90**:
690 628-653.
- 691 **Merret R, Carpentier M-C, Favory J-J, Picart C, Descombin J, Bousquet-Antonelli**
692 **C, Tillard P, Lejay L, Deragon J-M, Charng Y-y. 2017.** Heat shock protein
693 HSP101 affects the release of ribosomal protein mRNAs for recovery after heat
694 shock. *Plant Physiology* **174**: 1216-1225.
- 695 **Narsai R, Law SR, Carrie C, Xu L, Whelan J. 2011.** In-depth temporal transcriptome
696 profiling reveals a crucial developmental switch with roles for RNA processing and
697 organelle metabolism that are essential for germination in *Arabidopsis*. *Plant*
698 *Physiology* **157**: 1342-1362.

- 699 **Park SJ, Kwak KJ, Oh TR, Kim YO, Kang H. 2009.** Cold shock domain proteins affect
700 seed germination and growth of *Arabidopsis thaliana* under abiotic stress
701 conditions. *Plant and Cell Physiology* **50**: 869-878.
- 702 **Perino C, Côme D. 1991.** Physiological and metabolic study of the germination phases
703 in apple embryo. *Seed Science and Technology* **19**: 1-14.
- 704 **Raudvere U, Kolberg L, Kuzmin I, Arak T, Adler P, Peterson H, Vilo J. 2019.** g:
705 Profiler: a web server for functional enrichment analysis and conversions of gene
706 lists (2019 update). *Nucleic acids research* **47**: W191-W198.
- 707 **Reichel M, Liao Y, Rettel M, Ragan C, Evers M, Alleaume A-M, Horos R, Hentze
708 MW, Preiss T, Millar AA. 2016.** In planta determination of the mRNA-binding
709 proteome of *Arabidopsis* etiolated seedlings. *The Plant Cell* **28**: 2435-2452.
- 710 **Sablok G, Powell J, Kazan K. 2017.** Emerging roles and landscape of translating mRNAs
711 in plants. *Frontiers in Plant Science* **8**: 1443.
- 712 **Sajeev N, Bai B, Bentsink L. 2019.** Seeds: a unique system to study translational
713 regulation. *Trends in plant science* **24**: 487-495.
- 714 **Scheer H, de Almeida C, Ferrier E, Simonnot Q, Poirier L, Pflieger D, Sement FM,
715 Koechler S, Piermaria C, Krawczyk P. 2021.** The TUTase URT1 connects
716 decapping activators and prevents the accumulation of excessively deadenylated
717 mRNAs to avoid siRNA biogenesis. *Nature communications* **12**: 1-17.
- 718 **Soppe WJ, Bentsink L. 2020.** Seed dormancy back on track; its definition and regulation
719 by DOG1. *New Phytologist*.
- 720 **Sorenson R, Bailey-Serres J. 2014.** Selective mRNA sequestration by
721 OLIGOURIDYLATE-BINDING PROTEIN 1 contributes to translational control
722 during hypoxia in *Arabidopsis*. *Proceedings of the National Academy of Sciences*
723 **111**: 2373-2378.
- 724 **Tyanova S, Temu T, Sinitcyn P, Carlson A, Hein MY, Geiger T, Mann M, Cox J.
725 2016.** The Perseus computational platform for comprehensive analysis of (prote)
726 omics data. *Nature Methods* **13**: 731-740.
- 727 **Xiang Y, Nakabayashi K, Ding J, He F, Bentsink L, Soppe WJ. 2014.** Reduced
728 Dormancy5 encodes a protein phosphatase 2C that is required for seed dormancy
729 in *Arabidopsis*. *The Plant Cell* **26**(: 4362-4375.

730 **Xu J, Chua N-H. 2009.** Arabidopsis decapping 5 is required for mRNA decapping, P-
731 body formation, and translational repression during postembryonic development.
732 *The Plant Cell* **21**: 3270-3279.

733 **Xu J, Yang J-Y, Niu Q-W, Chua N-H. 2006.** Arabidopsis DCP2, DCP1, and VARICOSE
734 form a decapping complex required for postembryonic development. *The Plant*
735 *Cell* **18**: 3386-3398.

736 **Zhang Z, Boonen K, Ferrari P, Schoofs L, Janssens E, van Noort V, Rolland F,**
737 **Geuten K. 2016.** UV crosslinked mRNA-binding proteins captured from leaf
738 mesophyll protoplasts. *Plant Methods* **12**: 42.

739

740

741

For Peer Review

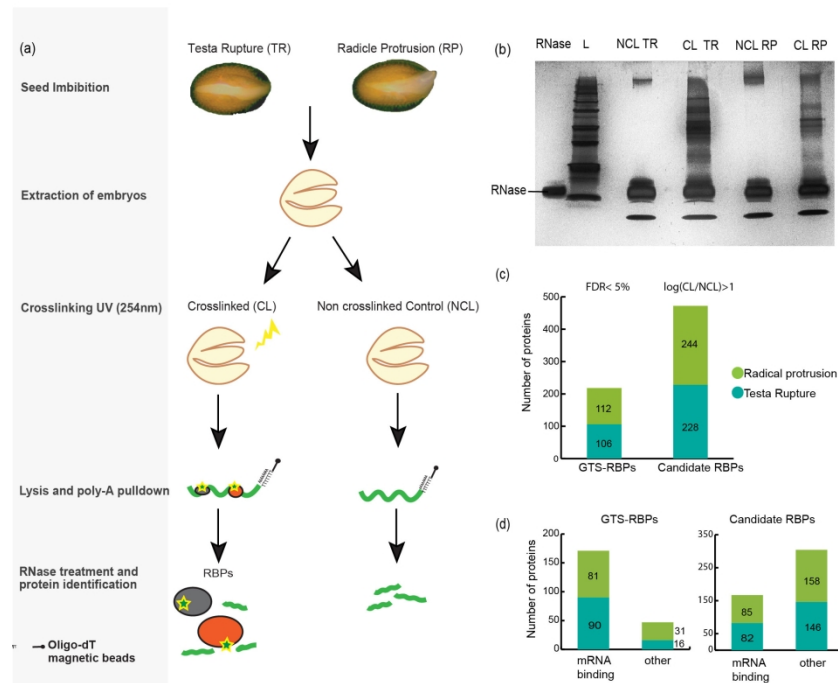


Fig. 1 mRNA interactome capture of the Arabidopsis germination translational shift. (a) Schematic representation of mRNA interactome capture at Testa rupture (TR) and Radicle protrusion (RP), the two stages that define the germination translational shift (GTS). (b) A silver stained SDS page gel showing the RNase enzyme control at the left side of the protein ladder (L) and to the right side are the mRNA-protein complexes that were isolated from the non-crosslinked (NCL) and crosslinked (CL) samples of the TR and RP stages. Results are representative of three independent interactome capture experiments with three biological replicates. (c) Bar graphs representing GTS-RBPs which were proteins identified with high confidence FDR<0.5 and candidate RBPs that show log₂(CL/NCL)>1 enrichment at TR and RP. (d) Categorization of the GTS-RBPs and candidate RBPs based on the Gene ontology term 'RNA binding'.

212x148mm (300 x 300 DPI)

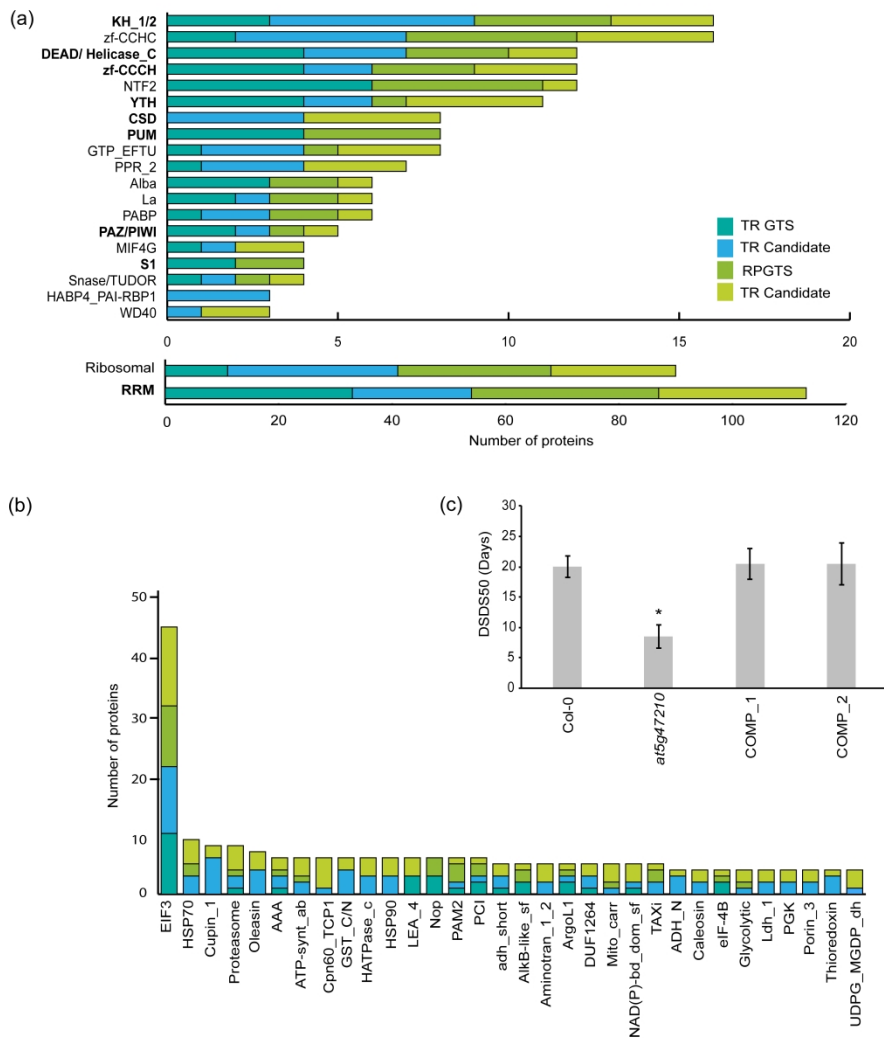


Fig. 2 Proteins domain classification of the identified GTS and candidate RBPs in the germination translational shift of *Arabidopsis thaliana*. (a) Classical and Non-classical RNA binding domains (RBDs) at Testa Rupture (TR) and Radicle protrusion (RP). The classical RBDs are indicated in bold (families with ≥ 3 proteins depicted in figure). (b) Putative RBDs at TR and RP (families with >4 proteins depicted in figure). (c) Graph representing the days of dry seed storage to reach 50% germination (DSDS50). A mutant of the hyaluronan/mRNA binding protein AT5G47210 (at5g47210) and two complementation lines (COMP_1 and COMP_2) were analysed for their DSDS50 compared to the wild-type Col-0 at 26°C. The results are representative averages of four biological replicates (SE, t-test, $p < 0,05$; error bar).

1979x2101mm (72 x 72 DPI)

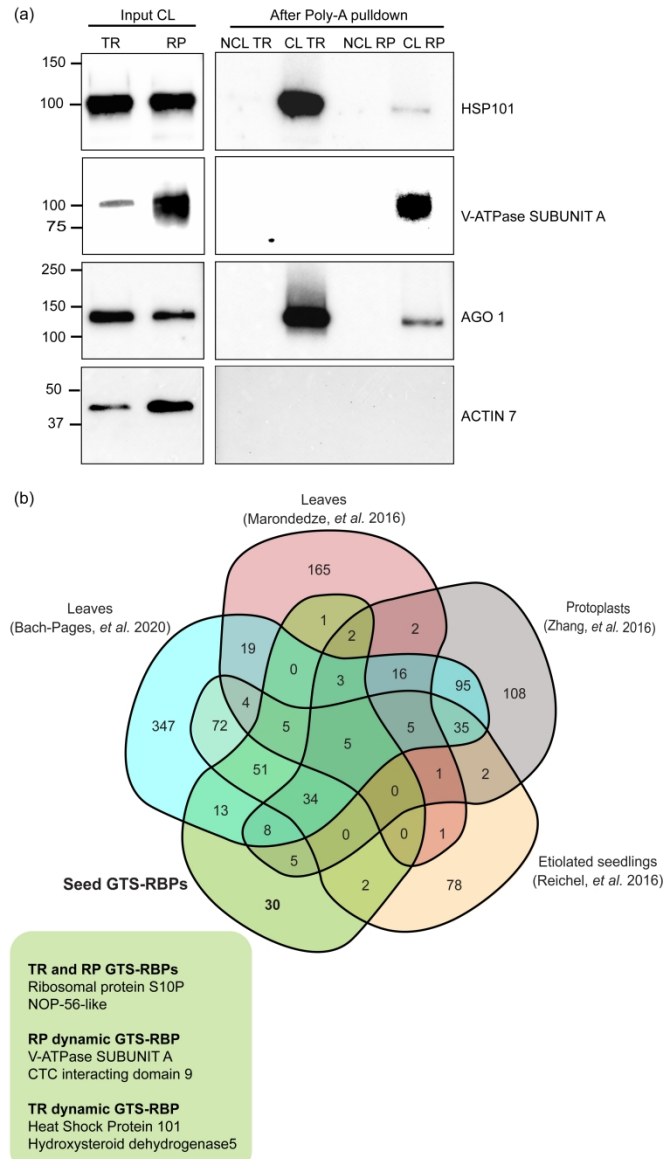


Fig. 3 Dynamic GTS-RBPs and seed specific RBPs identified during the germination translational shift of *Arabidopsis thaliana*. (a) Western blot image confirming the dynamic nature of GTS-RBPs HSP101 at the Testa rupture (TR) stage and V-ATPase subunit A at the Radicle protrusion (RP) stage after the poly-A pulldown. AGO1 was used as a known RBP control, while ACTIN 7 as a non-RBP negative control. The non-crosslinked (NCL) and crosslinked (CL) samples were normalized based on the mRNA quantity after the poly-A pulldown, while the total protein input for the CL samples were loaded with a fixed volume of the total protein from the CL lysates. (b) Venn Diagram comparing the GTS-RBPs identified in this study and previously performed mRNA interactome captures in different plant tissues. The green box shows representative seed specific GTS-RBPs that were either identified at both stages or dynamic for the Testa rupture (TR) or Radicle protrusion (RP) stages.

1108x1982mm (72 x 72 DPI)

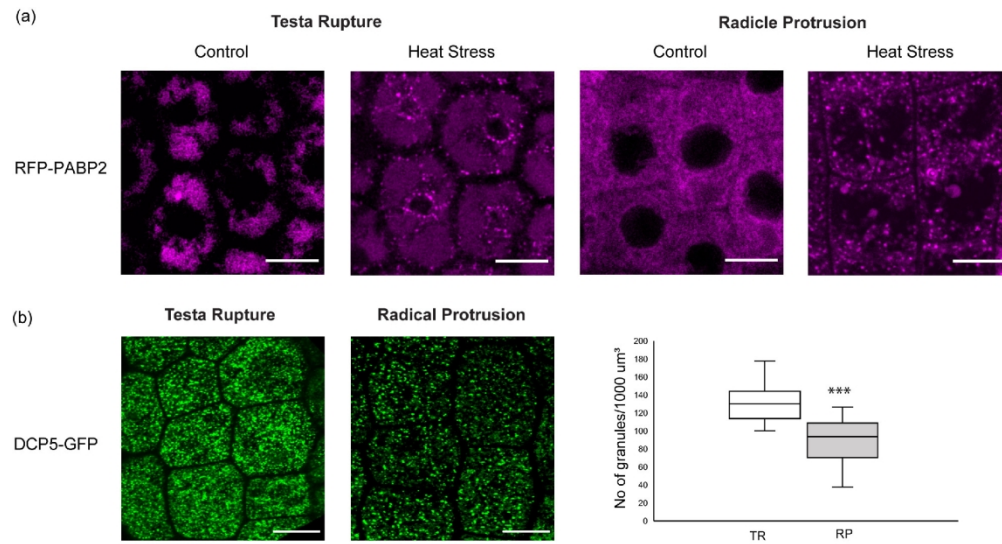


Fig. 4 Visualization of P-bodies and stress granules at the Testa rupture and Radicle protrusion stages of *Arabidopsis thaliana* seed germination. (a) Visualization of stress granules using dual reporter line pDCP1-YFP-DCP1/pPABP2-tRFP-PABP2 at TR (background bodies are large vacuoles commonly present at this stage) and RP at optimal germination conditions (control) or under short heat stress of 30 minutes at 42°C (b) Visualization of P-bodies using reporter line pUBQ-DCP5-GFP at radicle protrusion (RP) and testa rupture (TR). Box-plot showing the number of granules /1000 um. (n= 30 root epidermal cells and 5 embryos per stage, scale bar = 10 micron).

168x94mm (300 x 300 DPI)

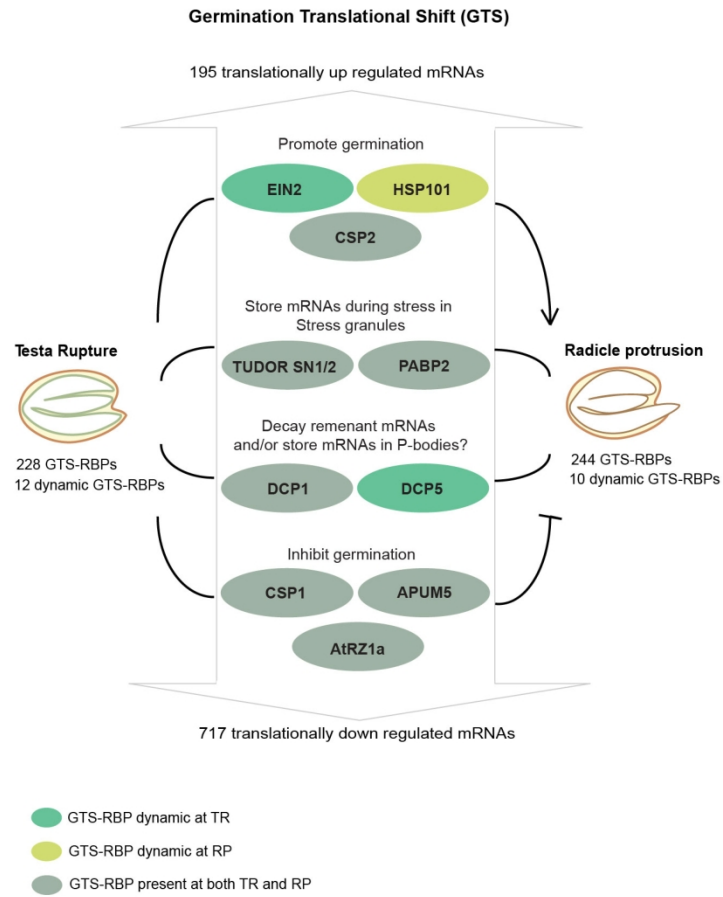


Fig. 5 Summary of the features at the Germination Translational Shift (GTS). The number of RNA binding proteins that are identified at testa rupture and radicle protrusion are indicated at the left and right side of the figure, respectively. The box in the middle of the figure presents the GTS-RBPs (ovals) that play a role in germination and may regulate the translational of mRNAs during the GTS. The numbers indicated in the top and bottom of the figure represent the mRNAs that are under translational control identified by Bai et al., 2017.

156x144mm (300 x 300 DPI)